Available online www.jsaer.com

***Journal of Scientific and Engineering Research*, 2018, 5(1):197-212**

Research Article

ISSN: 2394-2630
CODEN(USA): JSERBR

Three-Dimensional Computational Investigation of the Power Separation and Flow Anatomy in the Vortex Tube

Seif T. Abdelghany[1], Hamdy A. Kandil[2]

[1]Research Associate, Mechatronics Engineering Department, German University in Cairo, Egypt
[2]Associate Professor, Mechanical Engineering Department, Faculty of Engineering, Alexandria University, Egypt

Abstract A CFD study of the vortex tube is presented in this article using a three-dimensional (3D) model of the tube using ANSYS Fluent®. The 3D analysis of the flow is carried out to have a better visualization of the flow through the tube and to investigate its features.

The results showed the existence of two vortices moving in opposite axial directions with the same direction of rotation, and also the existence of a stagnation point after which there is no power separation in the tube.

The current study introduces a new theory of the vortex tube operation where the energy (power) separation inside the tube is in analogy with that in the gas refrigeration cycle (the reversed Brayton cycle). The inner vortex acting as a turbine, rotates the outer vortex that acts as a compressor and increases its power by transferring some of its angular momentum.

Keywords Ranque–Hilsch Vortex Tube, Vortex Tube (VT), Maxwell's Demon, Energy separation, Power Separation, ANSYS Fluent

Nomenclature

D	Vortex Tube diameter	m
d_c	Cold orifice diameter	m
L	Length of vortex Tube	m
Z	Axial distance along the tube	m
p	Pressure	Pa
T_{in}	Inlet Nozzle Temperature	K°
u	x-component of velocity vector	$m\ s^{-1}$
v	y-component of velocity vector	$m\ s^{-1}$
w	z-component of velocity vector	$m\ s^{-1}$
x	Cartesian x-coordinate	m
y	Cartesian y-coordinate	m
z	Cartesian z-coordinate	m
H	Total enthalpy	$Joule$
T	Static temperature	K°
G_κ	Generation of turbulence kinetic energy due to the mean velocity gradients	
G_b	Generation of turbulence kinetic energy due to buoyancy	
Y_M	Contribution of the fluctuating dilation in compressible turbulence to the overall dissipation rate	
S_κ, S_ε	User defined Source terms	

Greek Symbols

μ	Dynamic viscosity	$Pa\ s$
μ_c	Cold mass fraction	

υ	Specific volume	$m^3 kg^{-1}$
ν	Tangential component of the velocity	$m\ s^{-1}$
ρ	Density	$kg\ m^{-3}$
δ_{ij}	Kronecker delta function$\left(\delta_{ij} = 1\ if\ i = j\ and\ \delta_{ij} = 0\ if\ i \neq j\right)$	
τ_{ij}	Viscous stress tensor	
K	Turbulent kinetic energy	$m^2\ s^{-2}$
ε	Turbulent dissipation rate	$m^2\ s^{-3}$
$C_{1\varepsilon}$,$C_{2\varepsilon}$, $C_{3\varepsilon}$, C_μ	κ- εmodel constants	
σ_ε	Turbulent Prandtl number for ε	
σ_κ	Turbulent Prandtl number for κ	
μ_t	Turbulent (or eddy) viscosity	$Pa\ s$

1. Introduction

The vortex tube (VT) is a device with a simple geometry without any moving mechanical parts [1,2,3]. It enables the separation of hot and cold air vortices from the inlet compressed air that is tangentially supplied to the tube through the inlet nozzle(s) [4,5]. The vortex tube was first discovered in 1933 by the French physicist Georges J. Ranque [6], and in 1947 the German engineer Rudolf Hilsch [7] improved and modified the design of Ranque. The vortex tube consists of many parts [8,9] including; one or more inlet nozzles, a vortex chamber, a control valve or a plug that is located at the hot end, a cold end orifice and a working tube. When compressed air is injected tangentially through the inlet nozzles into the vortex chamber, a strong rotational flow field (vortex) is formed at the periphery of the tube wall. The vortex propagates until the end of the tube where some of the air leaves the tube via the hot outlet. However, adjusting the control valve at the hot outlet causes the rest of the air to reverse its direction and exit from the cold outlet along the centerline of the tube. It is noted that two vortices occur inside the tube, one at the periphery of the tube which exits at the hot outlet at a temperature much higher than the inlet temperature and another one at the core of the tube with opposite flow direction which exits at the cold orifice with a temperature much lower than the inlet temperature.

The VT is used in many applications such as cooling of airborne electronic components, cooling of gas samples, and cooling of soldered parts including spot welding and ultrasonic welding. It is also used in the separation of air into nitrogen and oxygen rich fluid stream [10,11]. The VT has many advantages [12,13,14] because of its low cost, light weight, reliability, compactness and free maintenance as it has no moving parts. It has an adjustable temperature range and cools without the use of any refrigerant or electricity.

2. Literature Review

A power separation between the cold and hot streams occurs inside the vortex tube which causes the temperature differences between the inlet and exit streams. Many researchers suggested various theories to explain the power separation inside the vortex tube. For example, Ahlborn [15,16] suggested that the RHVT is a refrigeration device that can be modeled and analyzed as a classic thermodynamic refrigeration cycle with significant temperature splitting, refrigerant and coolant loops, expansion and compression loops and heat exchangers. They reported that a secondary circulation exists inside the vortex tube and acts as a refrigerant to transfer the energy from the cold flow to the hot flow.Some researchers noted the existence of secondary circulations in the vortex tube. They attributed the energy separation to the secondary circulations. For example, Behara et al [17],using a 3D 60° sector model of the vortex tube confirmed the existence of secondary circulations inside the RHVT at small cold orifice to tube diameter ratio (d_c/D) and that such circulations become weak as the d_c/D ratio increases and they disappear at d_c/D ratios higher than 0.583. They showed that the total energy transfer was reduced by 21% due to the existence of secondary circulations. Therefore, they concluded that they can be considered as a performance degrading mechanism. Such conclusion was confirmed by Farouk [18,19] using a large eddy simulation (LES) of the VT which showed that the secondary circulation resulted in enhancing the mixing between cold and hot flows which increased the temperature of air exiting at

cold outlet. Also, Bovand et al [20] confirmed that the secondary circulations are a performance degrading mechanism.

Some researchers [21,1,22,23] reported that the energy separation inside the RHVT is due to work transfer caused by a torque produced by viscous shear between inner and outer flows..

The effect of friction and turbulence inside the VT has always been a major concern of many researchers and was considered by some researchers as the reason for power separation. For example, using a simple vortex tube model with CFX software and κ-ε turbulence model, Kazantseva et al [24] attributed the energy separation inside the VT to the energy and gas dynamic interaction of vortices inside the VT. Behara et al [25] modeled the RHVT using STAR-CD software and concluded that the energy separation inside the VT exists due to the shear work and heat transfer between the hot and cold streams. Bovand et al [20] studied a 3D model of the VT and concluded that a large portion of the energy transfer inside the RHVT is due to the tangential viscous shear. Aljuwayehl et al [1] explained the operation of the VT by the existence of viscous shear acting on a control rotating surface separating the cold and hot flow regions. A torque is produced which causes work transfer between the cold and hot flows. El May et al [26], using a 3D modeling of the RHVT, reported the formation of a great amount of tangential shear stress of the flow near the wall of the tube, and proposed that the tangential shear work can be considered the most important mechanism of energy separation in the tube.

Another theory for the power separation inside the RHVT was proposed by Xue et al [27,8,9] where the temperature drop of the cold stream is caused by the pressure gradient at the cold outlet of the tube where there is sudden expansion which is considered the main process for cold temperature drop. While, the temperature rise at the hot end is caused due to the multi circulations near the hot end where a partial stagnation is formed. These multi circulations are considered to be the main reason for increasing the hot outlet temperature as a result of viscous heating.

Kurosaka [28] attempted to explain the energy separation inside the VT by acoustic streaming. He proposed that the energy separation is due to damping of acoustic streaming

It is noted that until now there is no clear theory for the energy separation inside the RHVT, which requires further investigation of the flow topology and the physics of the vortices inside the tube.

Kandil and Abdelghany [29] attempted to enhance the performance of the VT by studying the effects of the length to tube diameter ratio(L/D) and the cold orifice to tube diameter ratio(d_c/D)on the performance of the tube. The current study will extend the analysis of the previous study [29]in an attempt to develop an operational theory of the tube.

Pourmahmoud et al [30,31] and Bramo et al [2,32] studied the stagnation point inside the RHVT and showed that the stagnation point can be characterized as either the point where the maximum wall temperature occurs or the point on the centerline of the tube where the axial velocity becomes zero. However, both researches showed that these two points do not coincide with each other. Both researchers studied the existence of the stagnation point at only one cold mass fraction (μ_c), which is the ratio between the cold outlet mass flow rate divided by the inlet mass flow rate, of 0.3.

The stagnation point and the parameters affecting its existence and location in the VT will be investigated in this study in an attempt to determine the optimum length of the tube.

3. Numerical Model

3.1. 3.1 Governing Equations

A3D CFD model of the RHVT was simulated using ANSYS Fluent® software based on the model developed by the authors [29]. ANSYS Fluent software solves the following compressible turbulent flow conservation of mass, momentum and energy and state equations [33] (ANSYS Fluent Theory Guide):

Continuity equation in tensor notation:

$$\frac{\partial \bar{\rho}}{\partial t} + \frac{\partial}{\partial x_j}\left(\bar{\rho}\bar{u}_j + \overline{\rho' u_j'}\right) = 0$$

$$j = 1,2,3$$

Momentum equations in tensor notations (all three components):

$$\frac{\partial}{\partial t}\left(\bar{\rho}\bar{u}_i + \overline{\rho' u_i'}\right) + \frac{\partial}{\partial x_j}\left(\bar{\rho}\bar{u}_i\bar{u}_j + \bar{u}_i\overline{\rho' u_j'}\right) = -\frac{\partial \bar{p}}{\partial x_i} + \frac{\partial}{\partial x_j}\left(\bar{\tau}_{ij} - \bar{u}_j\overline{\rho' u_i'} - \bar{\rho}\overline{u_i' u_j'} - \overline{\rho' u_i' u_j'}\right)$$

where

$$\bar{\tau}_{ij} = \mu\left[\left(\frac{\partial \bar{u}_i}{\partial x_j} + \frac{\partial \bar{u}_j}{\partial x_i}\right) - \frac{2}{3}\delta_{ij}\frac{\partial \bar{u}_k}{\partial x_k}\right]$$

Energy Equation:

$$\frac{\partial}{\partial t}\left(\bar{\rho}\bar{H} + \overline{\rho' H'}\right) + \frac{\partial}{\partial x_j}\left(\bar{\rho}\bar{u}_j\bar{H} + \bar{\rho}\overline{u_j' H'} + \overline{\rho' u_j'}\bar{H} + \overline{\rho' u_j' H'} + \bar{u}_j\overline{\rho' H'} - k\frac{\partial \bar{T}_i}{\partial x_j}\right)$$
$$= \frac{\partial \bar{\rho}}{\partial t} + \frac{\partial}{\partial x_j}\left[\bar{u}_i\left(-\frac{2}{3}\mu\delta_{ij}\frac{\partial \bar{u}_k}{\partial x_k}\right) + \mu\bar{u}_i\left(\frac{\partial \bar{u}_j}{\partial x_i} + \frac{\partial \bar{u}_i}{\partial x_j}\right) - \frac{2}{3}\mu\delta_{ij}\overline{u_i'\frac{\partial u_k'}{\partial x_k}} + \mu\left(\overline{u_i'\frac{\partial u_j'}{\partial x_i}} + \overline{u_i'\frac{\partial u_i'}{\partial x_j}}\right)\right]$$
$$i, j, k = 1,2,3$$

3.2. Turbulence Model

The current CFD model is based on the κ-ε Turbulence model which was used also in the previous study [29]. In the κ-ε Turbulence model, the Turbulent kinetic energy, κ, and it's rate of dissipation, ε, are obtained from the following transport equations [33]:

$$\frac{\partial}{\partial t}(\rho\kappa) + \frac{\partial}{\partial x_i}(\rho\kappa u_i) = \frac{\partial}{\partial x_j}\left[\left(\mu + \frac{\mu_t}{\sigma_\kappa}\right)\frac{\partial \kappa}{\partial x_j}\right] + G_\kappa + G_b - \rho\varepsilon - Y_M + S_\kappa$$

$$\frac{\partial}{\partial t}(\rho\varepsilon) + \frac{\partial}{\partial x_i}(\rho\varepsilon u_i) = \frac{\partial}{\partial x_j}\left[\left(\mu + \frac{\mu_t}{\sigma_\varepsilon}\right)\frac{\partial \varepsilon}{\partial x_j}\right] + C_{1\varepsilon}\frac{\varepsilon}{\kappa}(G_\kappa + C_{3\varepsilon}G_b) - C_{2\varepsilon}\rho\frac{\varepsilon^2}{\kappa} + S_\varepsilon$$

The turbulent (or eddy) viscosity, μ_t, is computed by combining κ and ε as follows:

$$\mu_t = \rho C_\mu \frac{\kappa^2}{\varepsilon}$$

The model constants. $C_{1\varepsilon}$,$C_{2\varepsilon}$, C_μ, σ_ε and σ_κ have the following default values:

$$C_{1\varepsilon} = 1.44,\ C_{2\varepsilon} = 1.92, C_\mu = 0.09,\ \sigma_\varepsilon = 1.3, \sigma_\kappa = 1.0$$

The results of the VT CFD model became mesh independent at 163,900 elements. Due to the complexity and sensitivity of the flow inside the VT the time step of the solution had to be very small such that the run time of the simulation ranged from 24 to 72 hours in extreme cold mass fraction cases using an 8 processors 3.64 GHz HP workstation Z800 with 16 GB Ram.

The geometry used in the current CFD model is based on the Exair™ 708 slpm vortex tube used by Skye et al [34] as shown in Figure 1

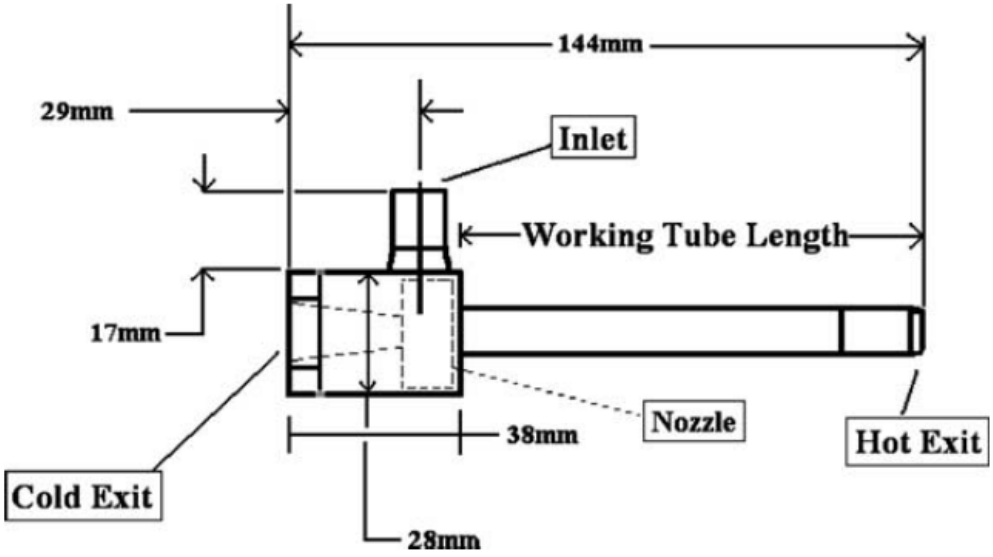

Figure 1: Schematic of the vortex tube used in the CFD model [34]

3.3. Boundary Conditions

The boundary conditions used in the current model were obtained from previous study [29] where:-

1) Inlet nozzles: Mass flow inlet boundary conditions with a mass flow rate of 8.35 g s^{-1}, and total temperature of 294.2 K
2) Cold outlet: Pressure outlet
3) Hot outlet: Pressure outlet
4) Tube Wall: No slip boundary conditions with adiabatic walls

3.4. Results

A case study at a cold mass fraction of 0.56 will be used to study the physics inside the vortex tube including the properties of the inner and outer vortices, the stagnation point and the theory of operation.

The total temperature contours in the VT at the current operating conditions are shown in Figure 2. It is noted from the results in Figure 2 that, as the air moves from the inlet towards the hot outlet, at the periphery of the tube, its total temperature increases to reach its maximum value at the hot outlet at the end of the tube. At the same time as the returning air moves along the core of the tube towards the cold outlet, its total temperature decreases to reach its minimum value at the cold outlet. Such system is very complicated as two vortices coexist in the tube with one exiting at a high temperature and the other one at a very low temperature. This system suggests that the energy lost by the cold vortex must be gained by the outer hot vortex. Such assumption requires that the two vortices must have the same direction of rotation and the must have an interaction mechanism to allow this kind of energy (power) transfer.

The nature of the inner and outer vortices and the interaction mechanism between the vortices and its relation to the power separation inside the tube are presented in the next sections

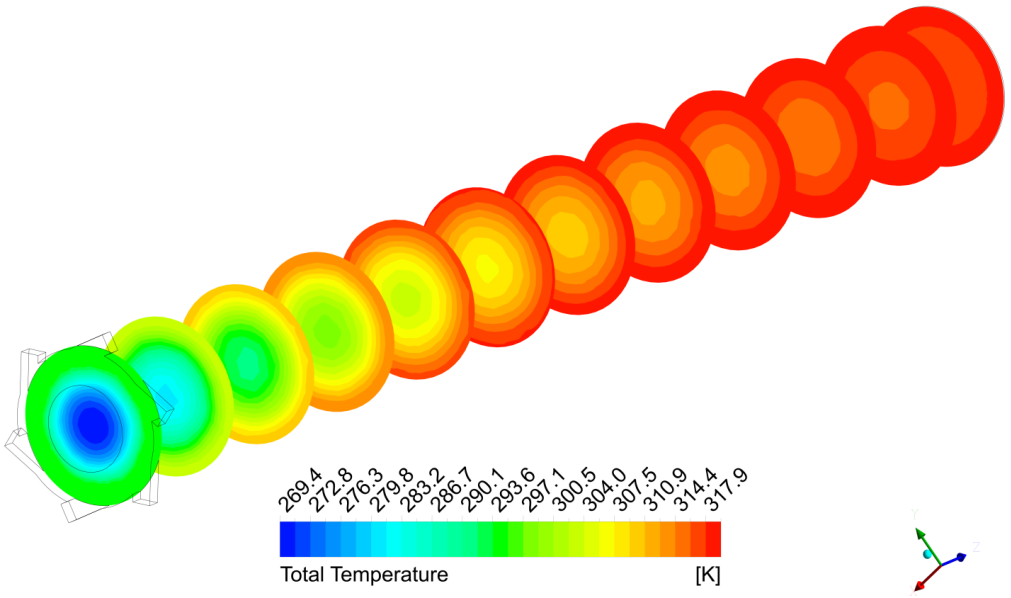

Figure 2: Total Temperature Contours Sections along the VT

4. 3D Physics of RHVT

The existence of inner and outer vortices was mentioned in the literature but such a mechanism cannot be easily observed experimentally and whether the direction of both vortices is the same or not was not cleared. The air flow starts at the inlet nozzles and due to the angle of entrance; a vortex is formed near the periphery of the tube where air moves towards the hot outlet. Part of the air, defined by the cold mass fraction, reverses its axial direction and moves towards the cold outlet forming an inner vortex. The inner vortex exits the tube at the cold outlet with a temperature much lower than the inlet air temperature while the outer vortex exits the tube at the hot outlet with a temperature higher than the inlet air temperature. Controlling the cold mass fraction controls the temperatures at both the cold and hot outlets.

It can be observed from Figure (a) that two vortices exist inside the RHVT. The location and direction of rotation of the inner vortex with respect to the outer vortex is shown in Figure 3 (b). The figure clearly shows that both vortices have the same direction of rotation

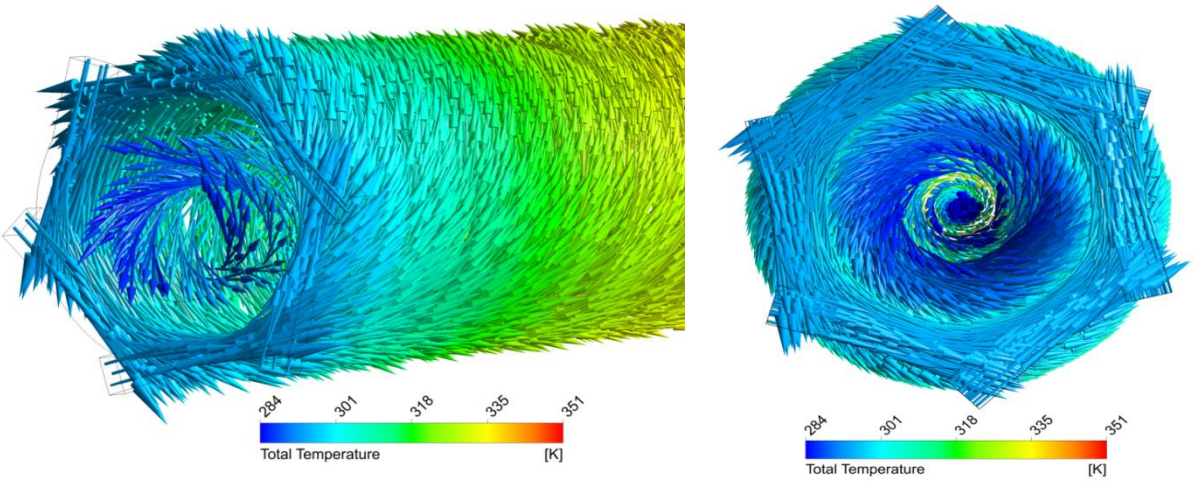

(a) (b)

Figure 3: 3D velocity vectors in the RHVT in (a) Isometric view and (b) Front view

Gustol and Kurosaka, as cited in [30], reported that a free vortex exists inside the vortex tube near the wall of the tube and, Xue [8] reported that a forced vortex is formed near the cold end of the tube. In order to confirm such observations the tangential velocity distributions along the radius of the RHVT at different axial positions is presented in Figure 4. Figure 4 shows the radial profile of the tangential velocity at different axial positions along the tube which has very high values near the wall of the tube and negligible values at the core. This indicates the existence of a free vortex near the wall of the tube and a forced vortex at the core of the tube. The tangential velocity near the tube core follows a solid-body rotation where the velocity increases with increasing the radius, $V \approx \omega r$. Noting that the cold stream moves in the negative direction of Z, the value of the rotational speed increases along the tube length such that the highest value exists at the smallest value of Z (Z/L = 0.01) while the lowest value exists at the largest value of Z (Z/L = 0.8). The tangential velocity near the tube periphery follows a free vortex behavior where the speed is inversely proportional to the radius such that the velocity reaches zero at the tube wall. The value of the rotational speed of the hot stream decreases along the tube length such that the highest value exists at the smallest value of Z while the lowest value exists at the largest value of Z.

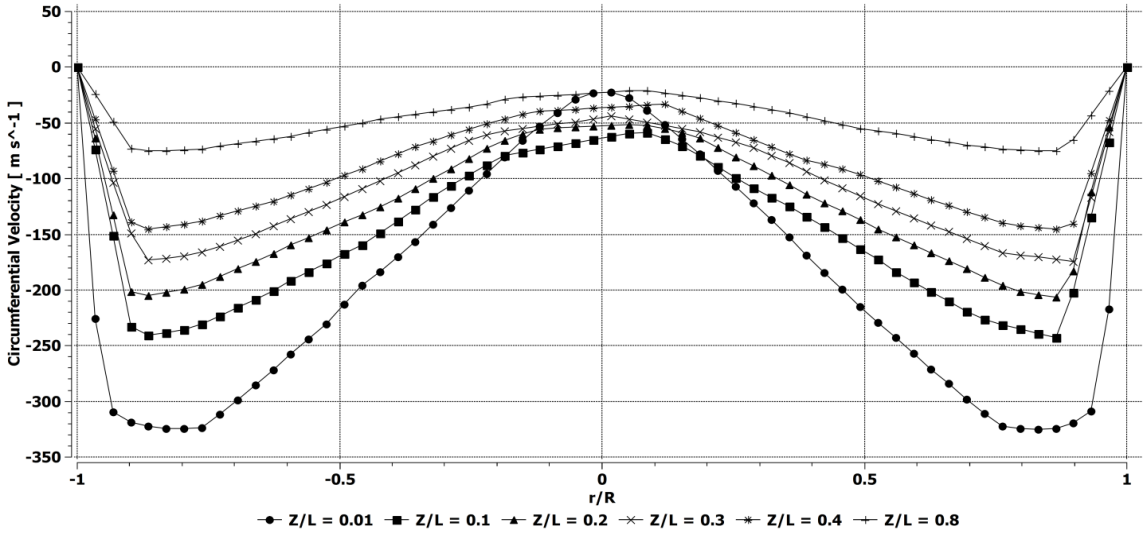

Figure 4: Radial Distribution of the Tangential velocity at different axial position

5. Stagnation Point inside the RHVT

Many researchers [25,20,35,2,32,30,31]reported the existence of a stagnation point inside the vortex tube and that it occurs in long tubes where the axial velocity of the air in the inner vortex becomes zero. The flow along center of the tube beyond this point is directed towards the hot outlet with no reverse flow. However, the intensive research applied on the stagnation point inside the RHVT as mentioned in the literature review was carried out at only one cold mass fraction of 0.3. Therefore, and in order to better understand the nature of the stagnation point and its existence, a 3D CFD model of a 230-mm length tube was simulated in this study. The results are compared with those of a similar 3D model of a 106-mm length tube at a cold mass fraction of 0.56 which was not used in the literature. The purpose of the simulation at a different cold mass fraction was to compare the results qualitatively with the previous results and to check if the concept and the characteristics of stagnation point will be the same at different cold mass fractions.

The radial distribution of the axial velocity at different axial positions along the tube length for the two tubes of 106 and 230-mm lengths both operating at a cold mass fraction of 0.56 with inlet mass flow rate of 8.35 g s^{-1} and inlet total temperature of 294.2 K are shown in Figure 5 and Figure 6. It is observed from the presented results that, in the tube of 106-mm length the stagnation point is located at the end of the tube where the axial velocity reaches zero, while in the 230-mm tube model the stagnation point is located at an axial position of Z/L = 0.5. After the stagnation point, the air along the center line of the tube changes its axial velocity direction from moving towards the cold outlet to moving towards the hot outlet at the end of the tube. The magnitude of the axial velocity increases as the air approaches the hot outlet.

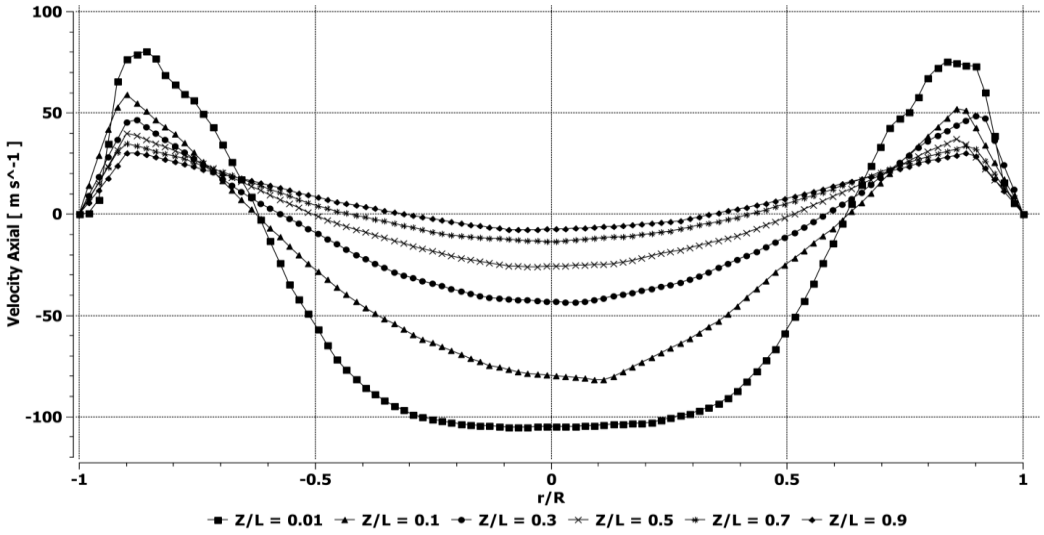

Figure 5: Radial distribution of the axial velocity at different axial positions for the 106 mm tube

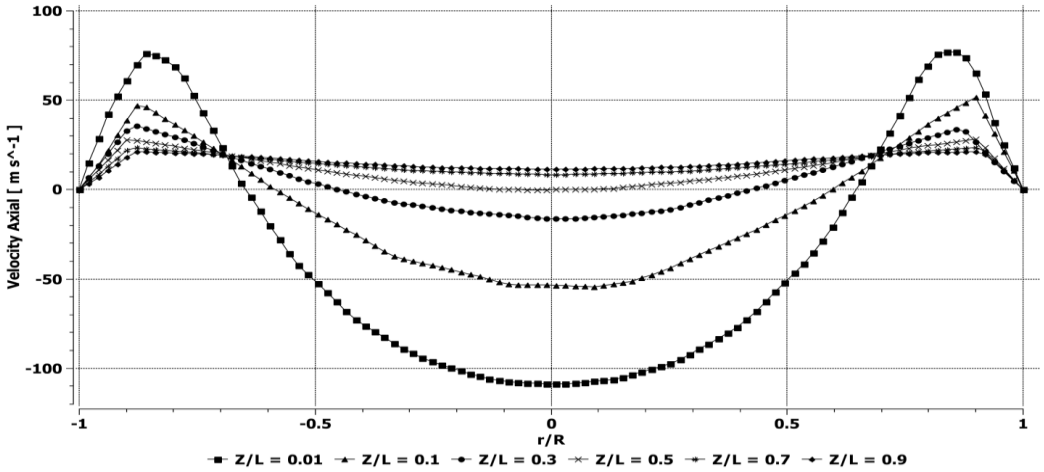

Figure 6: Radial distribution of the axial velocity at different axial positions for the 230 mm tube

The results on Figure 5 and Figure 6 show the expansion of the cold vortex core, and the location of the shear layer between the two vortices, with the direction of its motion where the largest core size exists at the smallest value of Z (Z/L=0.01).

Maurya [36] confirmed that increasing the length of the vortex tube beyond the stagnation point will lead to a very slight change in energy separation. This result was attributed to the existence of the stagnation point, which suggests that energy separation takes place only before the stagnation point. In order to investigate such a result, the total temperature along the diameter of the tube at different axial positions along the tube must be investigated.

The radial distribution of the total temperature at different axial positions along the tube for the tubes of lengths of 106 mm and 230 mm are shown in Figure 7 and Figure 8, respectively. It is observed from both Figures that the temperatures of the cold outlet of both models are very close and the same result applies to the hot outlets temperatures. This shows that further increase in the vortex tube length beyond the stagnation point has very slight effect on power separation. Also, the temperature in the 230-mm tube model becomes almost constant after the axial position of Z/L =0.5, which is the location of the stagnation point, as it was shown in Figure 6.

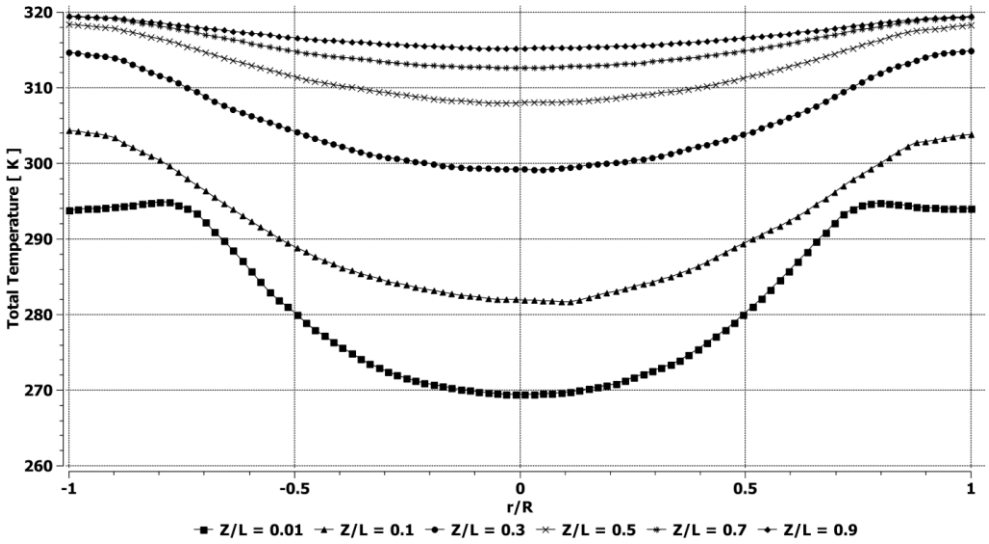

Figure 7: Radial distribution of the total temperature at different axial positions for the 106 mm tube

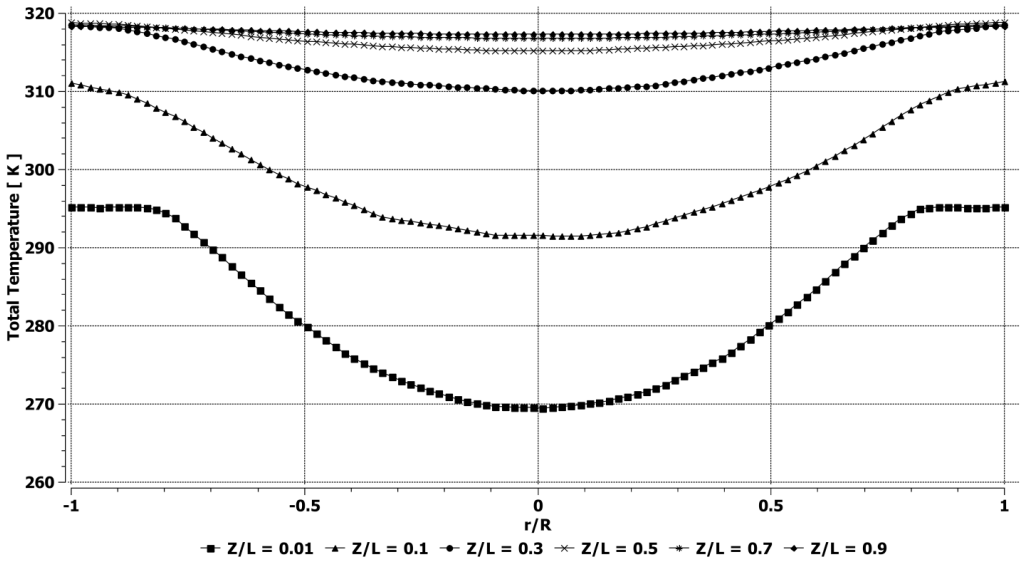

Figure 8: Radial distribution of the total temperature at different axial positions for the 230 mm tube

Figure 9 and Figure 10 show the total energy sections contours along the VTs of lengths of 230 mm and 106 mm, respectively. After the stagnation point only one flow stream exists in the tube moving towards the hot

outlet and there is no exchange of angular momentum. Only the friction at the wall of the tube continues which causes the reduction in the total energy of the outer vortex beyond the stagnation point.

In Figure 9 and Figure 10, it is shown that the total energy of the air along the tube beyond the stagnation point at the hot outlet of the 230-mm tube is much less than the total energy of air at the hot outlet of the 106-mm tube which shows that the stagnation point location before the hot outlet has an important effect on the total energy of air exiting from the tube.

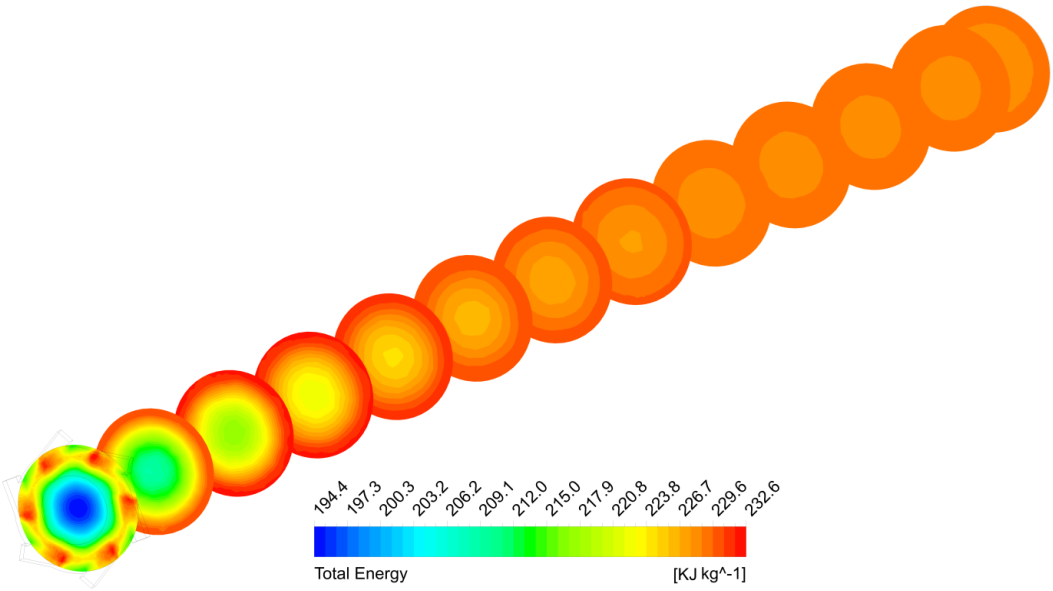

Figure 9: Total Energy section contours of RHVT of L =230 mm

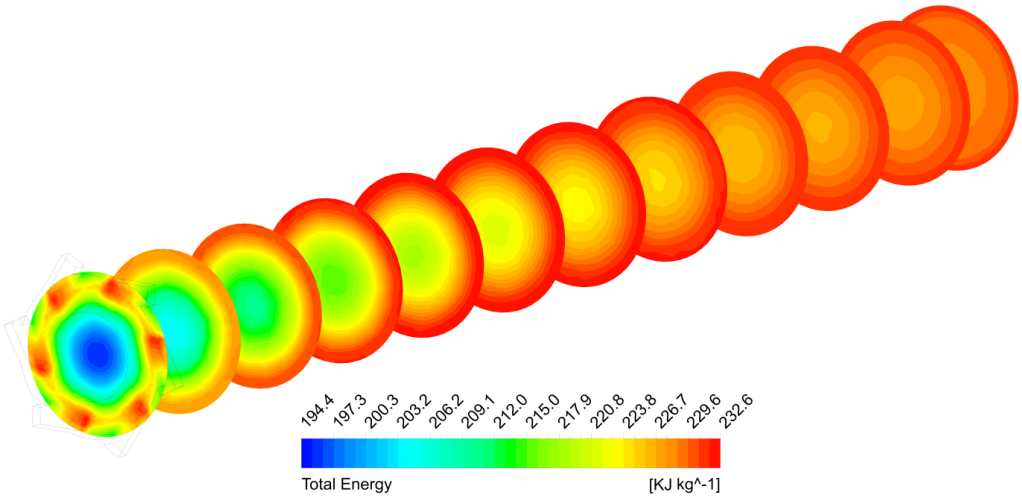

Figure 10: Total Energy section contours of RHVT of L =106 mm

6. Operational theory Physics of the RHVT.

In the gas refrigeration cycle (the reversed Brayton cycle), shown in Figure 11[37], the surroundings are maintained at constant temperature, T_o, and the refrigerated space is to be maintained at constant low temperature, T_L. The cycle starts at point 1 where the gas is compressed during process 1-2 (a compressor) and then the high pressure, high temperature gas at state 2 rejects heat to the surroundings which causes its temperature to drop toT_3 during the process 2-3 at constant pressure.

The gas then undergoes an expansion process in a turbine during process 3-4 where both the pressure and temperature drop. The gas temperature reaches T_4. During process 4-1 the gas absorbs energy from the refrigerated space at temperature T_o until the gas temperature rises to T_1.

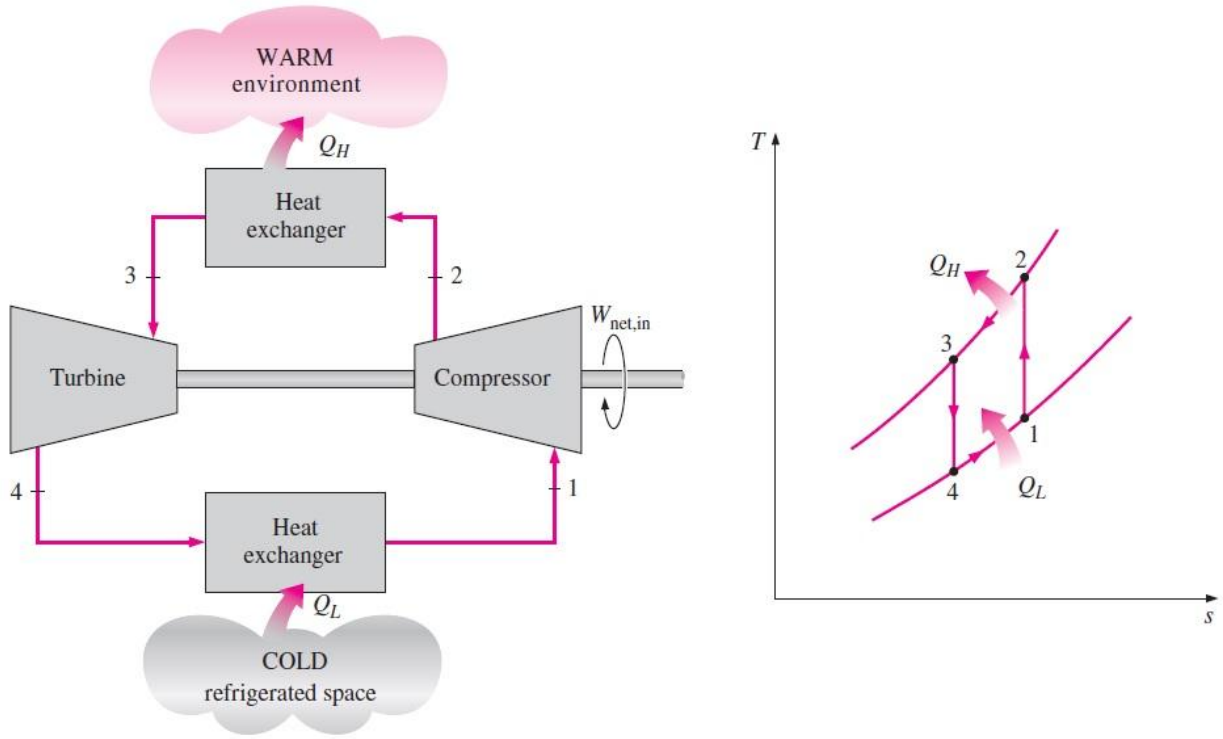

Figure 11: gas refrigeration cycle [37]

The power separation inside the RHVT can be modeled as a modified gas refrigeration cycle as shown in Figure 12.Air enters at the inlet of the tube at a temperature of T_{in} where it forms an outer vortex at the periphery of the tube at which it is compressed and it's temperature and pressure increase during process 1-2.As the hot outer vortex of air moves further along the tube it exchanges heat with the cold inner vortex during process 2-3.This part can be modeled as a heat exchanger where the heat is transferred from the hot outer vortex to the cold inner vortex. Part of the air of the outer vortex reverses it's axial direction and joins the core vortex. Such mass transfer occurs at many points as the outer vortex moves along the tube towards the hot outlet whereas the rest of the air exits the tube at the hot outlet at a temperature much higher than the inlet temperature. The air forming the inner vortex at the core of the vortex tube moves in an opposite axial direction to the outer vortex and it undergoes an expansion process like a turbine where it's temperature and pressure decrease during process 4-5. As the cold inner vortex moves towards the cold outlet, it exchanges heat with the outer vortex during process 5-6 to exit the tube at the cold outlet at a temperature much lower than the inlet temperature. As in the cycle of the gas refrigeration, part of the work of the cold vortex (core vortex) is transferred to the outer vortex.

The heat transfer from the hot outer vortex at the periphery of the tube and the cold inner vortex at the core of the tube doesn't enhance the power separation. On the contrary, it worsens the power separation as the hot vortex cools down and the cold vortex heats up. Therefore this heat transfer is not the reason behind the power separation in the VT.

It was confirmed in the 3D analysis of the VT in this study that the inner vortex and the outer vortex are rotating in the same direction. Therefore, the power separation in the tube can be explained by noting that the tube's operation is the same as the gas refrigeration cycle. The inner vortex at the core of the tube acts as an axial turbine and the outer vortex at the periphery of the tube acts as a compressor. The outer vortex (compressor) gains its power from the inlet air flow (input power) and the vortex at the core (turbine). The inner vortex rotation can be modeled as a solid body rotation which, by analogy to axial turbine, rotates the air at the periphery (compressor) which leads to increasing the energy and total temperature of the outer vortex and decreasing the energy and total temperature of the inner vortex. So, the power separation between both vortices

is by means of angular momentum where the solid body rotation of the inner vortex rotates the outer vortex and adds power to it which increases its energy and decreases the energy of the inner vortex. This can be interpreted in terms of the increase of the total temperature of the outer vortex and the decrease of the total temperature of the inner vortex.

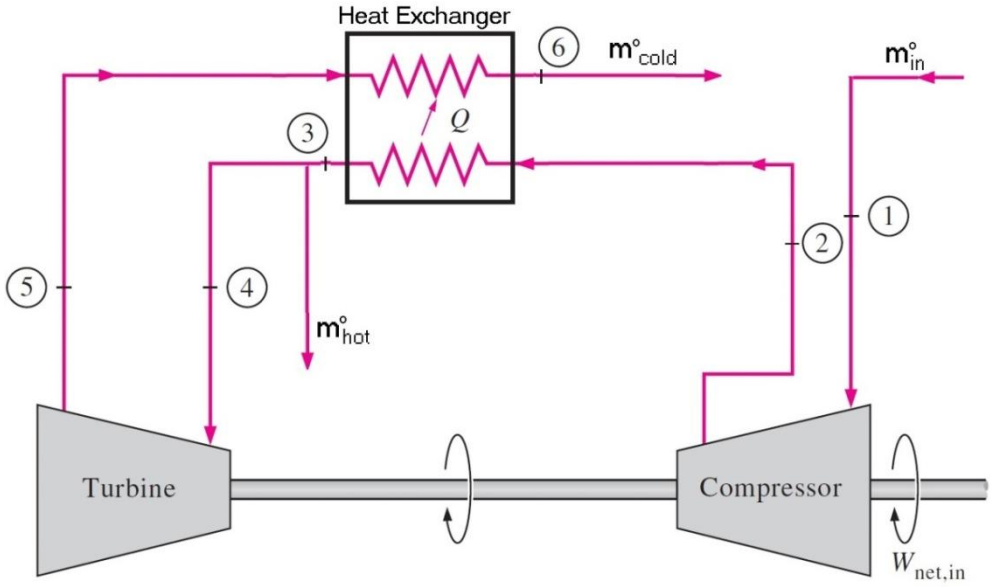

Figure 12: RHVT Modified Gas refrigeration cycle [37]

Studying the physics of the RHVT using a 3D model of inlet air flow rate of 8.35 gs^{-1} and total temperature of 294.2 °K at cold mass fraction of 0.5635 will provide a better understanding of the gas refrigeration cycle theory.

Figure 13 shows the radial distribution of total energy of air at different axial positions. The results in Figure 13 show that the energy of the outer vortex near the periphery of the tube is always larger than the energy of the inner vortex at the core of the tube at any axial position. The energy of the outer vortex increases as it moves towards the hot outlet, while the energy of the inner vortex decreases as the inner vortex moves towards the cold outlet which proves that the outer vortex is gaining part of its energy from the inner vortex.

Figure 14shows the axial distribution of the total energy of the air at different radial positions. The results show that the energy of the air near the periphery of the tube, r = 3,4 mm, (outer vortex) increases when moving toward the hot outlet which indicates the continuous energy gain from the inner vortex. At the pipe periphery (r = 5, 5.5 mm) the total energy increases until reaching almost the middle of the tube where the energy of the outer vortex starts decreasing as a result of losing energy in a form of friction with the pipe wall. The energy of the air at and near the tube core, r = 0-2 mm, (inner vortex) continuously decreases, as a result of transferring power to the outer vortex, to reach its minimum value at the cold outlet..

In the first part of the tube the power transfer in a form tangential angular momentum from the inner vortex to the outer vortex is more dominant which surpasses the heat transfer and the friction losses. The power transfer is resulting in the increase in the energy of the outer vortex and the decrease in energy of the inner vortex. While, when moving further along the tube the effect of the heat transfer from the outer vortex to the inner vortex and the friction with the tube walls surpass the tangential angular momentum effect which leads to the slight decrease in energy of the outer vortex at the periphery. The change of energy of the outer and inner vortices can be observed in Figure 15 which shows the total energy contours of the RHVT.

It can be observed from Figure that as the outer vortex moves towards the hot outlet the energy of the air starts to decreases near the hot exit which confirms that the effect of friction and the heat exchange between the inner and the outer vortex surpasses the effect of angular momentum transfer.

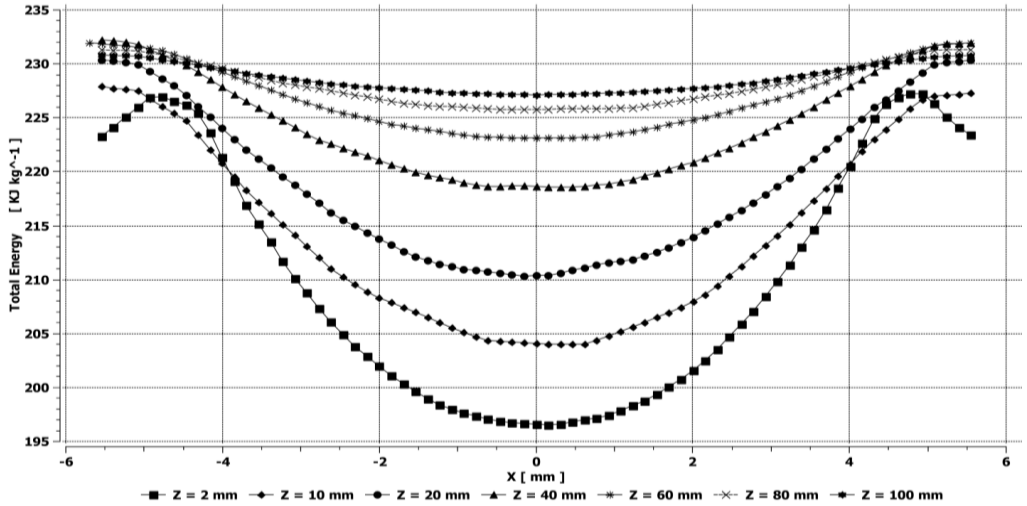

Figure 13: Radial distribution of the Total Energy at different Axial Positions

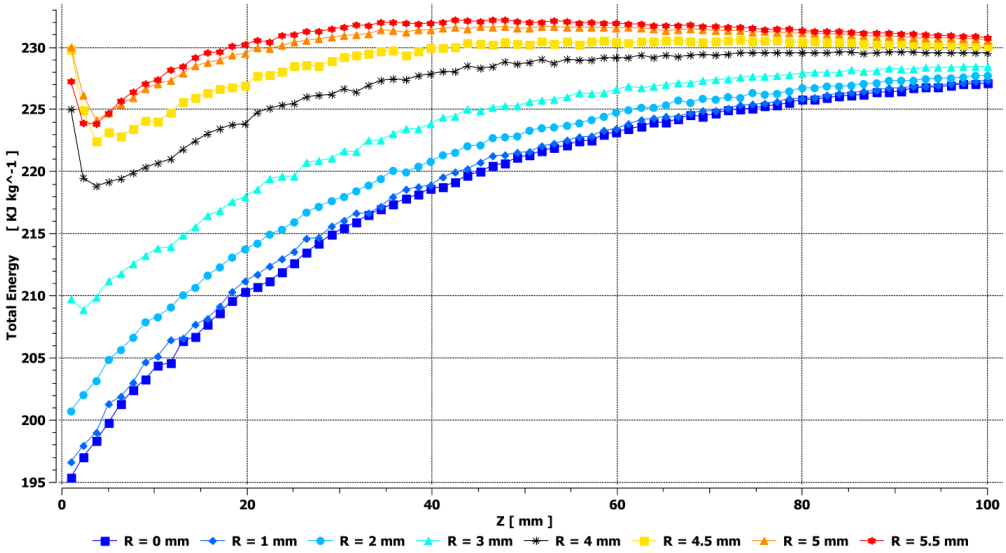

Figure 14: Axial distribution of the Total Energy at different Radial Positions

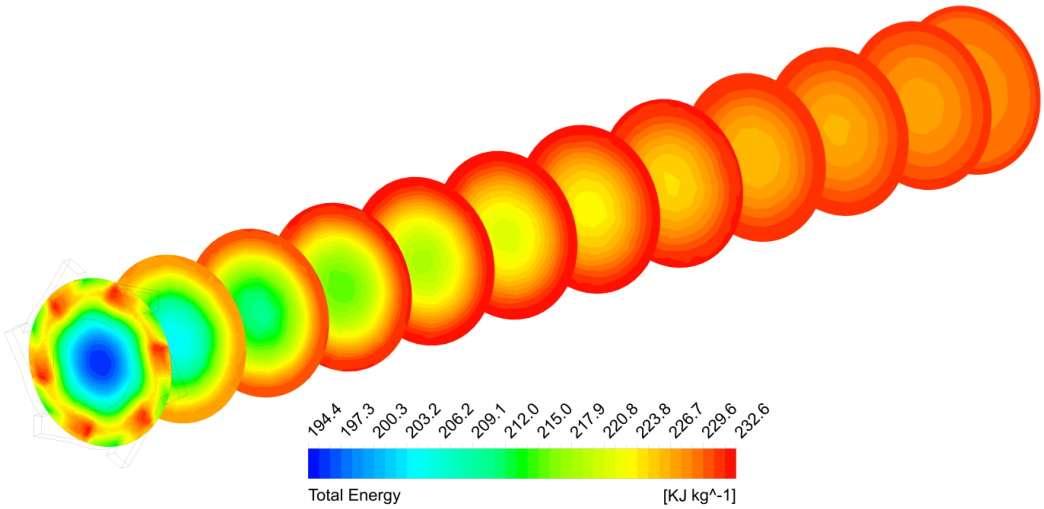

Figure 15: Total Energy Section Contours along the VT

In order for the inner vortex to move in an axial direction opposite to that of the outer vortex, a shear layer of zero axial velocity must exist between two vortices. This shear layer is shown as an iso-surface of zero axial

velocity in Figure 16. In Figure 16 it is shown that the shear layersize, where the axial velocity is equal to zero decreases when moving towards the hot outlet of the tube which indicates that the size of the inner vortex is increasing with the direction of its motion.

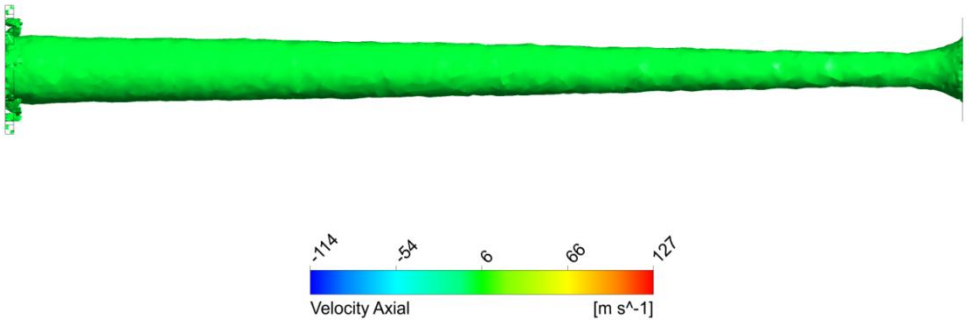

Figure 16: Iso-surface of zero axial velocity

For the inner vortex to be able to rotate the outer vortex and a transfer of angular momentum oto take place between the two vortices, the inner vortex must have higher vorticity than that of the outer vortex which is observed in Figure 17. The results in Figure 17 show that the inner vortex has much higher vorticity than that of the outer vortex which would explain how this tube can be modeled as turbo machine where the outer flow acts as a compressor and the inner vortex acts as an axial turbine. The inner vortex (turbine) transfers angular momentum to operate the compressor and this work can be viewed as energy loss by the inner vortex and energy gain by the outer vortex.

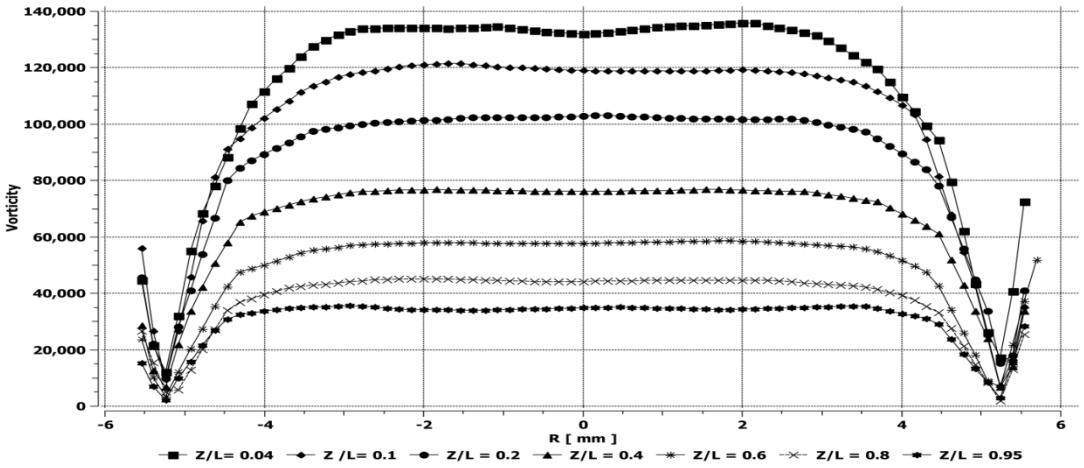

Figure 17: Vorticity distribution at different Axial Positions

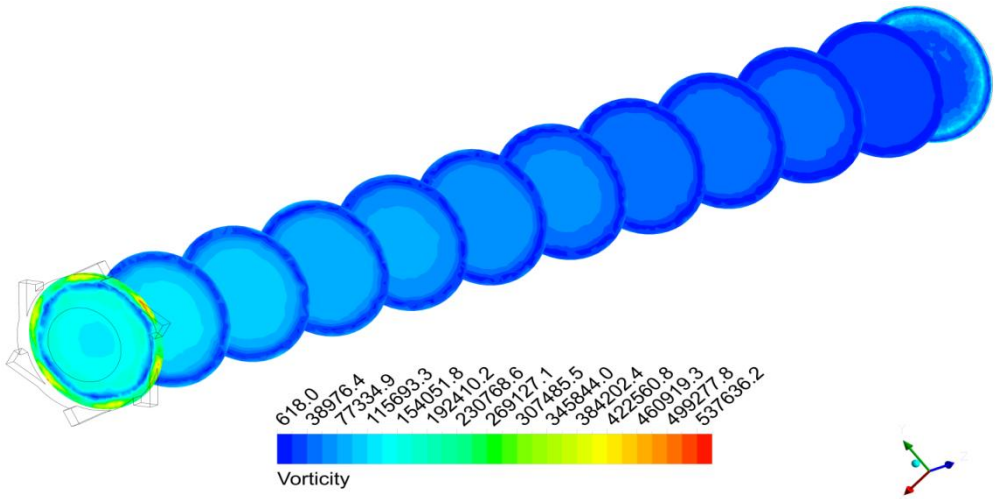

Figure 18: Vorticity Contours Sections along the VT

7. Conclusion

A three-dimensional computational model of the RHVT is used in this study in order to have better visualization of the flow in the tube and to investigate the physics of its operation.

The results of the current model showed the existence of two vortices inside the tube moving in opposite axial directions but rotating in the same direction of rotation. One vortex moves towards the hot outlet at the periphery of the tube and the other vortex moves towards the cold outlet along the centerline of the tube. The stagnation point existence along the centerline inside the tube was investigated as well and no power separation exits after it.

Finally the current study presented a new theory of operation for the RHVT which is in analogy to the gas refrigeration cycle (reversed Brayton cycle) where the inner vortex acts as a turbine, rotating the outer vortex which acts a compressor. The power transfer between both vortices in which the outer vortex gains energy and the inner vortex loses energy is based on the concept of the transfer of angular momentum between both vortices.

Acknowledgments

The support and allocation of the Computational facilities of the German University in Cairo (GUC) are gratefully acknowledged and appreciated.

References

[1]. N.F. Aljuwayhel, G.F. Nellis, and S.A. Klein, "Parametric and internal study of the vortex tube using a CFD model," *International Journal of Refrigeration*, vol. 28, pp. 442-450, 2005.

[2]. A. Bramo and N. Pourmahmoud, "A Numerical Study on the Effect of Length to Diameter Ratio and Stagnation Point on the Performance of Counter Flow Ranque-hilsch Vortex Tubes," *Australian Journal of Basic and Applied Sciences*, vol. 4, no. 10, pp. 4943-4957, 2010.

[3]. S. U. Nimbalkar and M. R. Muller, "An experimental investigation of the optimum geometry for the cold end orifice of a vortex tube," *Applied Thermal Engineering*, vol. 29, pp. 509-5014, 2009.

[4]. T. Dutta, K. P. Sinhamahapatra, and S. S. Bandyopdhyay, "Comparison of different turbulence models in predicting the temperature separation in a Ranque–Hilsch vortex tube," *International Journal of Refrigeration*, vol. 33, pp. 783-792, 2010.

[5]. O. Aydin, B. Markal, and M. Avci, "A new vortex generator geometry for a counter-flow RanqueeHilsch vortex tube," *Applied Thermal Engineering*, vol. 30, pp. 2505-2511, 2010.

[6]. G. J. Ranque, "Methods and Apparatus for Obtaining from a Fluid under Pressure Two Currents of Fluids at Different Temperatures," Patent 1,952,281, March 27, 1933.

[7]. R. Hilsch, "The Use of the Expansion of Gases in a Centrifugal Field as Cooling Process ," *The Review of Scientific Instruments*, vol. 18, no. 2, pp. 108-113, February 1947.

[8]. Y. Xue, M. Arjomandi, and R. Kelso, "Energy analysis within a vortex tube," *Experimental Thermal and Fluid Science*, vol. 52, pp. 139-145, 2014.

[9]. Y. Xue, M. Arjomandi, and R. Kelso, "Experimental study of the flow structure in a counter flow Ranque–Hilsch vortex tube," *International Journal of Heat and Mass Transfer*, vol. 55, pp. 5853-5860, 2012.

[10]. A. M. Crocker, S. M. White, and F. Bremer Jr., "Experimental Results of a Vortex Tube Air Separator for Advanced Space Transportation," in *in Proceedings of the 39th Joint Propulsion Conference and Exhibit,AIAA*, Huntsville, Ala, USA, 2003, p. 4451.

[11]. V. Balepin and D. Rosholt, "Progress in air seperation with the Vortex Tube," in *in Proceedings of the 9th international space planes and hypersonic systems and technologies conference* , Norfolk, Virginia, 1999, p. 4884.

[12]. S. Y. Im and S. S. Yu, "Effects of geometric parameters on the separated air flow temperature of a vortex tube for design optimization," *Energy*, vol. 37, pp. 154-160, 2012.

[13]. K. K. Zin, A. Hansske, and F. Ziegler, "Modeling and Optimization of the Vortex Tube with Computational Fluid Dynamic Analysis," *Energy Research Journal*, vol. 1, no. 2, pp. 193-196, 2010.

[14]. C. M. Gao, K. J. Bosschaart, J. C.H. Zeegers, and A. T.A.M. de Waele, "Experimental study on a simple Ranque–Hilsch vortex tube," *Cryogenics*, vol. 45, pp. 173-183, 2005.

[15]. B. K. Ahlborn and J. M. Gordon, "The vortex tube as a classic thermodynamic refrigeration cycle," *Journal of Applied Physics*, vol. 88, no. 6, pp. 3645-3653, September 2000.

[16]. B. K. Ahlborn, J. U. Keller, and E. Rebhan, "The Heat Pump in a Vortex Tube," *Journal of Non Equilibrium Thermodynamics*, vol. 23, pp. 159 - 165, 1998.

[17]. U. Behera et al., "CFD analysis and experimental investigations towards optimizing the parameters of Ranque–Hilsch vortex tube," *International Journal of Heat and Mass Transfer*, vol. 48, pp. 1961-1973, 2005.

[18]. T. Farouk and B. Farouk, "Large eddy simulations of the flow field and temperature separation in the Ranque–Hilsch vortex tube," *International Journal of Heat and Mass Transfer*, vol. 50, pp. 4724 - 4735, 2007.

[19]. T. Farouk, B. Farouk, and A. Gustol, "Simulation of gas species and temperature separation in the counter-flow Ranque–Hilsch vortex tube using the large eddy simulation technique," *International Journal of Heat and Mass Transfer*, vol. 52, pp. 3320 - 3333, 2009.

[20]. M. Bovand, M. S. Valipour, S. Eiamsa-ard, and A. Tamayol, "Numerical analysis for curved vortex tube optimization," *International Communications in Heat and Mass Transfer*, vol. 50, pp. 98-107, 2014.

[21]. C. Gao, "Experimental Study on The Ranque-Hilsch Vortex Tube," Technische Universiteit Eindhoven, Eindhoven, Ph.D. Thesis 2005.

[22]. V. A. Arbuzov, Y. N. Dubnishchev, A. V. Lebedev, M. Kh. Pravdina, and N. I. Yavorskii, "Observation of large-scale hydrodynamic structures in a vortex tube and the Ranque effect," *Tech. Phys. Lett.*, vol. 23, no. 12, pp. 938-940, 1997.

[23]. S. A. Colgate and J. R. Buchler, "Coherent transport of angular momentum – the Ranque–Hilsch tube a paradigm," in *14th Florida Workshop in Nonlinear Astronomy and PHysics, "Astrophysical Turbulence and Convection" Annuals of the New York Academy of Sciences*, New York, 2000.

[24]. O. V. Kazantseva, Sh. A. Piralishvili, and A. A. Fuzeeva, "Numerical Simulation of Swirling Flows in Vortex Tubes," *High Temperature* , vol. 43, no. 4, pp. 608-613, 2005.

[25]. U. Behera, P J Paul, K Dinesh, and S Jacob, "Numerical investigations on flow behaviour and energy separation in Ranque–Hilsch vortex tube," *International Journal of Heat and Mass Transfer*, vol. 51, pp. 6077-6089, 2008.

[26]. O. T. El May, I. Mokni, H. Mhiri, and P. Bournot, "CFD investigation of a vortex tube: Effect of the cold end orifice in the temperature separation mechanism," *Science Academy Transactions on Renewable Energy Ststems Engineering and Technology*, vol. 1, no. 3, pp. 84-89, September 2011.

[27]. Y. Xue, M. Arjomandi, and R. Kelso, "A critical review of temperature separation in a vortex tube," *Experimental Thermal and Fluid Science*, vol. 34, pp. 1367-1374, 2010.

[28]. M. Kurosaka, "Acoustic streaming in swirling flow and the Ranque–Hilsch (vortex-tube) effect," *Journal of Fluid Mechanics*, vol. 124, pp. 139-172, 1982.

[29]. Hamdy A. Kandil and Seif T. Abdelghany, "Computational Investigation of different effects on the performance of the Ranque-Hilsch Vortex tube," *Energy*, 2015.

[30]. N. Pourmahmoud and A. Bramo, "The effect of L/D ratio on the temperature separation in the counterflow vortex tube," *International Journal of Research and Reviews in Applied Sciences* , vol. 6, no. 1, pp. 60 - 68, January 2011.

[31]. N. Pourmahmoud, M. Rahimi, S. Rafiee, and A. Hassanzadeh, "A Numerical Simulation of The Effect of Inlet Gas Temperature on The Energy Separation in a Vortex Tube," *Journal of Engineering Science and*

Technology, vol. 9, no. 1, pp. 81 - 96, 2014.

[32]. A. Bramo and N. Pourmahmoud, "Computational fluid dynamics simulation of length to diameter ratio effect on the energy seperation in a vortex tube," *Thermal Science*, vol. 15, no. 3, pp. 833-848, 2011.

[33]. (2014, June) ANSYS - Fluent. [Online]. http://www.ansys.com/Products/Simulation+Technology/Fluid+Dynamics/Fluid+Dynamics+Products/ANSYS+Fluent

[34]. H.M. Skye, G.F. Nellis , and S.A. Klein, "Comparison of CFD analysis to empirical data in a commercial vortex tube," *International Journal of Refrigeration* , vol. 29, pp. 71-80, 2006.

[35]. M. Yilamz, M. Kaya, S. Karagoz, and S. Erdogan, "A review on design criteria for vortex tubes," *Heat and Mass Transfer*, vol. 45, pp. 613 - 632, 2009.

[36]. R. S. Maurya and K. Y. Bhavsar, "Energy and Flow Separation in the Vortex Tube : A Numerical Investigation," *International Journal on Theoretical and Applied Reseaech in Mechanical Engineering*, vol. 2, no. 3, pp. 25-32, 2013.

[37]. Yunus A. Cengel and Michael A. Boles, *Thermodynamics An Engineering Approach*, 4th ed. New York, United States of America: McGraw Hill, 2002.